Resilience assessment in post-wildfire recovery of road transport networks by dynamic thresholds and characteristic curves

Arango, Erica; Nogal, Maria; Yang, Ming; Sousa, Hélder S.; Matos, José C.; Stewart, Mark G.

DOI
10.1016/j.ress.2025.111365

Publication date
2025

Document Version
Final published version

Published in
Reliability Engineering and System Safety

Citation (APA)
Arango, E., Nogal, M., Yang, M., Sousa, H. S., Matos, J. C., & Stewart, M. G. (2025). Resilience assessment in post-wildfire recovery of road transport networks by dynamic thresholds and characteristic curves. *Reliability Engineering and System Safety*, *264*, Article 111365. https://doi.org/10.1016/j.ress.2025.111365

Reliability Engineering and System Safety 264 (2025) 111365

Contents lists available at ScienceDirect

Reliability Engineering and System Safety

journal homepage: www.elsevier.com/locate/ress

Resilience assessment in post-wildfire recovery of road transport networks by dynamic thresholds and characteristic curves

Erica Arango [b,*], Maria Nogal [b], Ming Yang [c], Hélder S. Sousa [a], José C. Matos [a], Mark G. Stewart [d]

[a] Department of Civil Engineering, ISISE, ARISE, University of Minho, Guimarães, 4800-058, Portugal
[b] Department of Materials, Mechanics, Management, and Design, Technical University of Delft, Delft, 2629, The Netherlands
[c] Department of Values, Technology, and Innovation, Technical University of Delft, Delft, 2629, The Netherlands
[d] School of Civil and Environmental Engineering, University of Technology Sydney, NSW, 2007, Australia

ARTICLE INFO

Keywords:
Resilience
Recovery
Road traffic networks
Wildfires
Extreme events

ABSTRACT

Understanding and enhancing the resilience of transport networks against climate-induced extreme events, such as wildfires, is critical to minimizing disruptions and their societal impacts. In this context, resilience is essential for effectively coping with these hazards, as road disruptions can hinder evacuation efforts, reduce accessibility, and lead to significant economic losses. Despite scientific progress, existing resilience assessment frameworks have limitations, including scenario-specific results and limited consideration of the underlying resilience concepts. To address these limitations, this paper introduces a resilience framework based on dynamic thresholds and characteristic curves to evaluate system recovery capacity. The framework incorporates a temporal dimension, allowing for the analysis of recovery time and recovery rate, which depend on the resources available for recovery activities. The characteristic curves illustrate system resilience by capturing key information on the preparedness, response, and recovery capacities inherent in each network. Consequently, the framework offers a more comprehensive view of system behavior during the recovery stage, as demonstrated through its application to a Portuguese case study. The insights gained can assist stakeholders in determining the feasibility of strengthening system resilience through enhanced response and recovery efforts, as well as in identifying when it is critical to reinforce resilience at earlier stages through adaptation measures.

1. Introduction

Societal impacts from wildfires have become a significant concern of the decade, with new records broken annually in terms of burned areas and the number of fires globally. For instance, in 2023, wildfires in Greece were declared the largest in the EU, resulting in over 20 casualties [1]. The total damage from wildfires in the European Union in 2023 reached approximately €4.1 billion ($4.43 billion) [2], affecting around 120.000 people [3]. Maui, Hawaii in 2023 faced one of the deadliest wildfires on record in the world, with at least 115 confirmed deaths and 388 people missing [4]. In addition, 3.000 structures were reported destroyed [5], of which 1.900 were homes. These damages represent a significant economic loss, and an initial estimate suggests that $5.5 billion will be required to address the damage in West Maui [6]. Concurrently, Los Angeles, California (2025), has experienced its worst fire season on record, resulting in 30 fatalities and the destruction of more than 16,000 structures [7].

Events like these create a context where critical infrastructures are often affected, with transportation systems being particularly vulnerable [8]. Transportation networks are vital for the daily functioning of society, playing a crucial role in the mobility of people and goods. Road networks, in particular, are an immediate necessity during disasters, as they are essential for evacuation and post-event recovery efforts [9]. Disruptive events can lead to challenges in post-disaster response, including difficult evacuation, accessibility issues, increased travel costs, and severe economic losses. This problem has been widely addressed from the perspective of transportation resilience, as it provides a holistic perspective on the functioning of transportation networks during and after unexpected events [10]. Especially as climate change leads to more frequent and unexpected extreme events, resulting in significant human and financial costs [8].

Resilience is defined as "the ability to prepare and plan for, absorb, recover from, or more successfully adapt to actual or potential adverse events" [11]. Transportation resilience is often assessed in terms of the

* Corresponding author.
E-mail addresses: E.A.Arango@tudelft.nl, ericaaarango@gmail.com (E. Arango).

https://doi.org/10.1016/j.ress.2025.111365

Available online 29 June 2025

system's recovery capacity (e.g., [12–19]). The resilience curve is one of the most widely used approaches for assessing systemic recovery, particularly in critical infrastructure systems during and after events [20]. These curves represent the relationship between the recovery time and some functionality measured through indicators such as network users (e.g., [21–23]), link flow (e.g., [24]), travel time reliability (e.g., [25–27]). Alternatively, recovery ratio, as an indicator, is also used to measure recovery resilience (e.g. [21,28]).

These recovery analyses have at least one of the following limitations:

(i) Case-dependent evaluations: Many assessments are scenario-based, making it impractical to explore all potential damage scenarios due to high computational costs. This lack of comprehensive analysis hinders the ability to draw generalized conclusions [29] and complicates comparisons between different networks and conditions.

(ii) Simplified system functionality: These models typically focus on a single performance indicator, such as passenger delay, travel time, or connectivity. However, considering only one indicator is insufficient to fully understand system behavior. Transportation networks serve multiple critical functions, such as safety, connectivity, and reliability, that are interdependent. Focusing solely on one indicator can overlook how these functions interact during disruptions. A comprehensive assessment using multiple indicators is essential to accurately evaluate system resilience and performance.

(iii) Descriptive approaches: Recovery is often studied from a descriptive perspective (i.e., assessing the recovery process) while neglecting the normative aspect (i.e., determining to what extent the recovery is acceptable). The normative approach is require to determine whether recovery performance meets acceptable standards.

(iv) Essential system characteristics: The recovery process is influenced by several factors, including available resources, hazard characteristics, and the extent of damage. This makes developing meaningful recovery estimations highly challenging [30]. These complexities align with the limitations outlined in (i) and (ii), hinder a comprehensive understanding of recovery dynamics. Furthermore, a lack of deep system understanding, such as the interactions between various components and how they collectively affect recovery, further complicates the creation of accurate and predictive recovery models.

(v) Recovery is not resilience: studying resilience solely in terms of recovery capacity presents a limited understanding of the concept. The recovery process is intrinsically linked to the system's ability to manage a specified level of damage. Ignoring the interrelationship between preparedness and recovery capacity constrains the decision-making process. This understanding is crucial for effectively managing the recovery process in communities [31].

While some studies address specific limitations, none provide a framework that tackles all the five issues simultaneously. For instance, [32] addresses Issue (i) by using Monte Carlo simulations to generate multiple damage scenarios. Similarly, the framework proposed in [33] mitigates Issues (i) to (iii) by assessing the preparedness level of a system (e.g., a road traffic network) exposed to wildfires of varying intensities, ranging from normal to extreme events. The framework assesses system performance across various functionalities, considering their importance and evaluating them based on an allowable performance loss. The permissible performance loss is contingent on both the hazard intensity and the functionality significance. Dynamic thresholds are employed for this assessment, enabling the evaluation of different states in a degradation process induced by escalating hazard intensities. Nonetheless, the framework does not currently evaluate the recovery process nor allow conclusions about the system's ability to recover.

Therefore, this paper aims to extend the existing framework to incorporate recovery assessment. To overcome all the limitations listed above and align with the proposed framework, the key contributions of this work include (i) extending the preparedness framework for recovery assessment by adding the time domain to full or partial recovery, while maintaining important aspects such as case-independent evaluation, multiple system functionalities and normative approach considering dynamic threshold. (ii) It identifies system's characteristic curves for recovery, which offer deeper insight by capturing essential system traits. These curves are system-specific and remain independent of damage scenarios and recovery resource allocation decisions. (iii) The framework considers the interrelationship between preparedness and recovery capacity of the system. Its application in a Portuguese case study demonstrates the framework's effectiveness in evaluating recovery.

The rest of the document is organized as follows: Section 2 outlines the fundamental principles of the existing preparedness assessment methodology. Section 3 delves into the description of the methodology extended to recovery assessment, including the characteristic curves. In Section 4, the framework is applied to a case study, with detailed decision-oriented discussion of the results. Finally, Section 5 presents conclusions.

2. Foundations: Preparedness assessment through dynamic thresholds

The framework proposed by Arango et al. [33] examines the performance of a traffic network across multiple functions, including safety, connectivity, reliability, and efficiency. The normative approach is introduced by juxtaposed the performance of each of these functions with their corresponding dynamic thresholds to obtain the capacity to cope with different hazard intensities, and, finally, a resilience index is obtained. The dynamic thresholds represent the acceptable performance losses, determined by the hazard intensity and the importance of the functionalities for the network's overall performance. Fig. 1a depicts the concept of dynamic thresholds in comparison to static thresholds. While static thresholds set a minimum requirement for system performance regardless of hazard intensity (in Fig. 1a, after point b, the system fails), dynamic thresholds adjust this minimum requirement based on the hazard intensity. For example, in Fig. 1a, under a dynamic threshold, the performance between points a and b is not acceptable for normal conditions, but after point c the it would be acceptable for high-intensity hazards. The reasoning behind dynamic thresholds is that, for instance, responding to a strike does not demand the same level of performance from the system as responding to a tsunami, just as a low-intensity fire does not required the same response as an extreme wildfire. It is noted that non-compliance with these thresholds does not necessarily indicate a system failure.

This framework is employed to assess the resilience of road networks in terms of their anticipatory and absorptive capacity, i.e., the network's preparedness. Accordingly, the approach proposes a specific formulation to assess how a traffic network's safety, connectivity, reliability, and efficiency are influenced by varying wildfire intensities. However, the recovery stage, i.e., post-event, is not addressed. Therefore, this paper presents the framework's extension to assess the recovery stage while retaining three essential elements of the approach: (i) a range of increasing hazard intensities; (ii) network functionalities (referred to as targets) organized into different levels of importance; and (iii) dynamic thresholds, associated with the hazard intensities and the importance of the functionalities. This is schematically depicted in Fig. 1b. For a detailed explanation of these elements and the complete framework to assess the preparedness of road traffic networks affected by different intensities of wildfire hazards, the reader is referred to [33].

The extension of this methodology to the recovery stage is not straightforward because the recovery stage includes more aspects to be considered, such as the different damage scenarios, the available resources, and the evolution of the recovery over time.

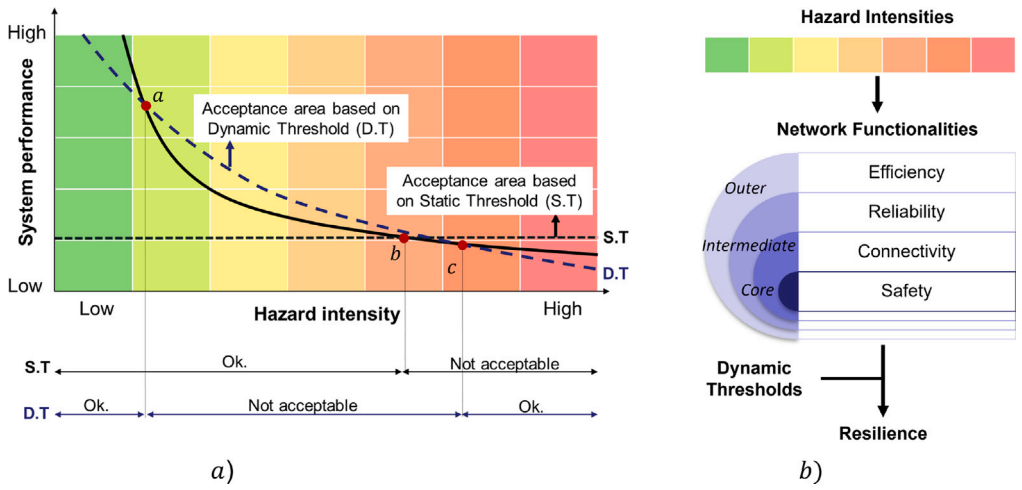

Fig. 1. Foundations of the framework: (a) Conceptual representation of dynamic thresholds. (b) Resilience evaluation through dynamic thresholds. *Source:* [33].

3. Recovery capacity assessment

This section explains how the methodology proposed by Arango et al. [33] is extended for evaluating the recovery of a system impacted by different levels of wildfire damage. The assessment of the recovery capacity consists of the performance evaluation of a road transport network as a function of recovery time and recovery rate for diverse damage levels. The performance of the network is obtained by evaluating its functionalities or targets during the recovery stage, e.g., safety, connectivity, and reliability.

Information from a single scenario is insufficient to fully capture the performance of an entire traffic network. Thus, based on the preparedness foundations, the proposed approach enables the exploration of multiple damage scenarios, offering a more comprehensive understanding of the network's performance during the recovery stage. Since each network has distinct characteristics and levels of preparedness, their recovery capabilities differ.

New aspects added to the original framework to allow recovery assessment are (i) the introduction of indicators to quantify the levels of damage and available resources; and (ii) the introduction of a temporal dimension to evaluate the change of the targets over time. The entire framework to assess recovery resilience is depicted in Fig. 2, highlighting the novel elements introduced into the existing framework to evaluate the recovery process.

The relevant aspects of the framework, both existing and new, are explained in detail below.

3.1. Damage assessment

Damage assessment depends on the specific hazard. In this case, the process is explained in the context of wildfire hazards affecting road transport infrastructures. To understand the recovery process in the context of wildfires, there are a few key stages that can be outlined as follows: 1- active wildfire, 2- suppression, 3- suppression repair, 4- emergency stabilization, and 5- long-term restoration. Stages 2 to 5 are conditioned by the intensity and magnitude of the fire, i.e., conditions of Stage 1. Note that the recovery activities are initiated once the hazard no longer affects directly the system, it could be from Stage 3 when the fire is under control. This highlights that the recovery process can begin even before the hazard is completely gone. In any case, it is important to carefully consider the stages of recovery and the appropriate actions. In this study, recovery activities are considered to start post-fire, when the damage can be quantified. Therefore, recovery assessment is concentrated in Stages 3 and 4.

Wildfires can damage road infrastructures directly and indirectly. According to Setunge et al. [34] direct impacts are the closure of roads, either due to surrounding fires during the event or falling objects that obstruct mobility after the disruptive event. In addition, prolonged exposure to fire and high intensities could lead to the degradation of the structural or functional capacity of roads, bridges, or other infrastructure and, eventually, to failure. Indirect impacts encompass damage to the surrounding area, such as the loss of stability, which can trigger additional hazards like landslides and erosion; the danger of falling trees, and the potential risk of flooding. This study focuses on the direct impacts of wildfires on road transportation networks. This is for two reasons; (i) road closures due to obstructions are more frequent than damage to infrastructure after a wildfire. For instance, only 2.8% of the bridges exposed to wildfires in the US have collapsed due to fires [35]; (ii) The study of multi-cascading hazards is beyond the scope of this paper.

3.1.1. Damage susceptibility and damage severity

After a wildfire, roads can become obstructed by burned debris, abandoned vehicles, fallen trees, and downed power lines. These blockages can lead to delays in carrying out emergency and recovery activities following wildfires. For instance, in the wildfires on Vancouver Island in 2023, the trees fell onto Highway 4 because their roots had been compromised [36], which resulted in the closure of the only paved road to the island's west coast communities of Port Alberni, Tofino, and Ucluelet. Also, in Australia in 2020, hundreds of people had to wait more than 10 h to evacuate due to falling trees and power poles [37]. Weakened trees along roads, known as hazard trees, can unpredictably fall on people and cars, resulting in injuries, fatalities, or hindrances to firefighting efforts. The biggest problem with hazard trees is that they can fail immediately after the wildfire or in the following months or years. Therefore, roads should not be opened to road users until the effect of these hazardous trees is mitigated. In that sense, removing hazard trees from roadways improves safety and access for road users, restoration and recovery projects, and emergency personnel. The mitigation of these trees should focus on roads where hazardous trees pose a risk to people's safety, property, or infrastructure. However, all forest areas affected by a wildfire are vulnerable to hazardous trees [38].

Building on this, damage assessment involves two key concepts: damage susceptibility and damage severity. In this context, susceptibility refers to the extent to which certain road segments are prone to damage. This can be calculated using various methods; however, in this case, it is determined by the presence of nearby trees and power lines that could obstruct specific sections of the road.

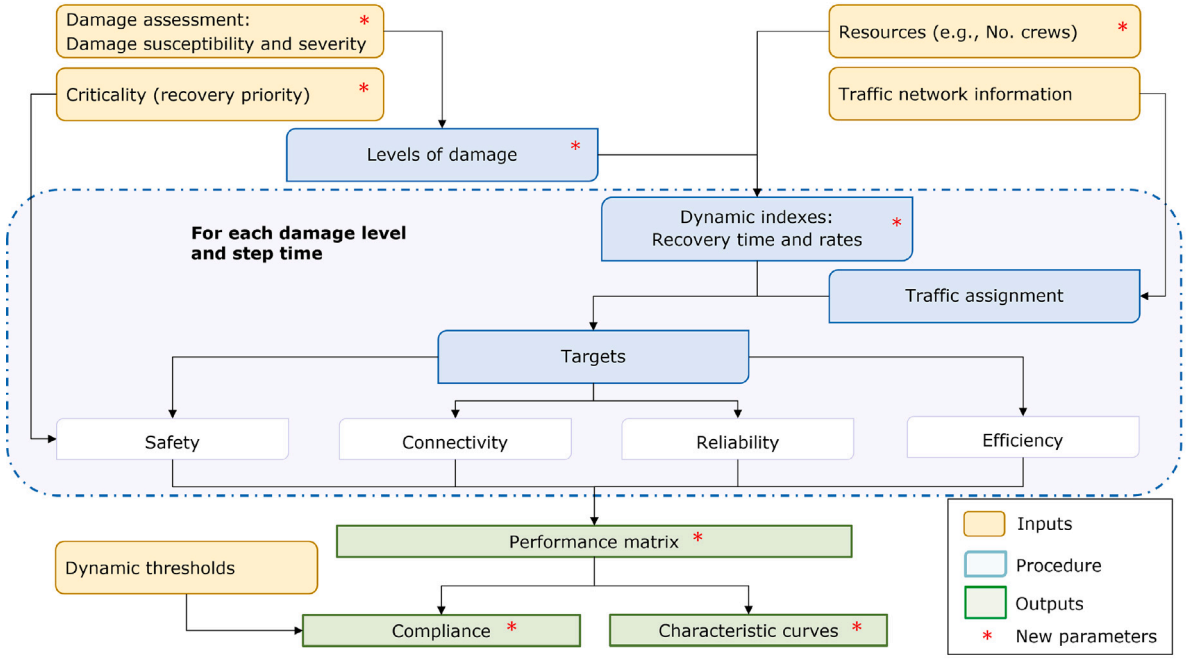

Fig. 2. Methodology for recovery assessment of a traffic network affected by diverse damage levels through dynamic thresholds and characteristic curves. Asterisks (*) indicate the new elements introduced into the framework in [33].

Table 1
Steps for damage assessment.

Step	Description
1. Identifying hazardous elements	Determine the target of study (e.g., roads, bridges) and the hazardous elements (e.g., trees, power lines in the case of wildfires).
2. Mapping susceptibility	Determine the susceptibility zone surrounding the target based on hazard-specific parameters (e.g., tree height for wildfires, floodplain boundaries for flooding). This can be done by using geospatial data (e.g., land use, vegetation, infrastructure maps) or remote assessments (e.g., satellite imagery, Google Maps, forensic reports).
3. Classifying damage severity	Define severity levels based on historical disasters or expert judgment to categorize damage intensity. In this study seven levels are considered, from negligible to extremely severe.
4. Damage assessment	Combine susceptibility and severity information to estimate the impact for each damage severity level. For instance, the number of fallen trees, or power poles affecting each km of road per damage level. This information is then use for recovery planning and resource allocation.

On the other hand, damage severity refers to the intensity of damage. For this, different levels of damage are defined to analyze the behavior of the system for a more complete damage range. In this case, seven damage levels are considered, namely: negligible, minor, moderate, medium, medium to severe, severe, and extremely severe. Technically, these seven levels of damage correspond to the seven categories of wildfire intensities used in the preparedness assessment.

The damage susceptibility and severity assessment follows the steps listed in Table 1.

Note that the inherent vulnerabilities of the roads themselves, such as pavement properties and structural layout, are not fully considered in this analysis, as explained in [39]. Instead, the study emphasizes varying levels of damage and susceptibility to wildfire hazards. While this methodology is explained in the context of wildfires affecting roads, it can be adapted for various hazards and infrastructures.

3.2. Recovery time and recovery rate

The recovery of road networks after a disruptive event depends on multiple factors, including the extent of damage, available resources, and prioritization criteria. There are two key dynamic indices used in the assessment for this purpose, recovery time and recovery rate. While recovery time refers to the time required to fully restore the functionality of a system, recovery rate is a measure of recovery trajectory. In this sense, the recovery rate can be expressed by the number of roads recovered per time unit, i.e., roads/h. These indices depend on the extent of damage and the resources available for recovery. Resources refer to all the available means that contribute to the recovery of the damage suffered, namely, economic, technical, and human resources.

As depicted in Fig. 3, the recovery assessment begins by defining recovery priorities based on the criticality of road segments and identifying available recovery resources, such as the number of response crews and their working capacity. Once priorities and resources are established, the recovery time for each road segment is computed by considering the severity of damage and the efficiency of available crews. Each damage level requires a different allocation of recovery resources, leading to variations in recovery time. Based on this information, the recovery rate is calculated as the number of roads restored per unit of time. Finally, the system functionalities are updated reflecting the recovery process. This will reflect how quickly different functionalities are restored.

Further explanations on recovery priorities and the assessment of various system functionalities are provided in the following subsections.

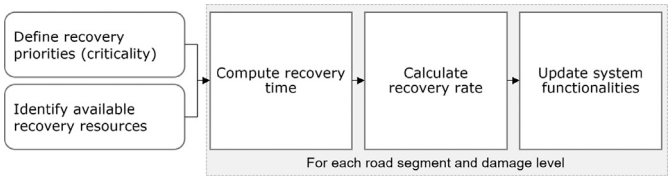

Fig. 3. Recovery time and recovery rate methodology.

3.2.1. Recovery priorities

After a shock, i.e., a sudden, intense, and often unexpected event that can cause significant and immediate disruptions to the road network, the primary goal is to quickly restore the affected areas of the system to a functional state. However, recovery resources are often limited, especially in cases involving extensive areas or multiple affected locations. Consequently, it can be challenging to simultaneously recover all areas of the system. For instance, during the recovery phase of a significant incident affecting various traffic routes, the highest priority is given to roads connecting to emergency services or those with the highest traffic volume, essentially, the most frequently used routes. To guide recovery prioritization decisions, a criticality parameter is introduced. This parameter emphasizes that more critical roads are related to more severe consequences when affected (e.g., social, economic, environmental, and health impacts) [40], making their quick recovery a top priority.

3.3. Targets in relation to recovery capacity

The target functions under consideration encompass safety, connectivity, reliability, and efficiency. These factors are considered in a hierarchical manner, where connectivity depends on safety, and reliability and efficiency are dependent on connectivity. These targets have been chosen to cover various domains in a resilience assessment. Safety and connectivity pertain to the physical domain, encompassing network infrastructure and other tangible components of the traffic network. Reliability and efficiency delve into the managerial domain, delineating traveler preferences, and the social domain, concerning the demand for road transport. The assessment of these targets across different levels of damage ($l \in \mathcal{L}$) is carried out through the formulation presented below, which takes into account damage indicators, traffic-related conditions, and resources.

The traffic network is represented by a set of nodes and a set of directed roads connecting those nodes, $i \in \mathcal{N}$. Several routes, denoted as $r \in \mathcal{R}_{pq}$ connect different origin–destination (OD) nodes, $pq \in \mathcal{PQ}$. The traffic demand from some OD pairs is known, and the traffic flow is distributed according to a traffic assignment model, e.g., the User Equilibrium model, that optimizes the travel time experienced by the drivers. A volume-delay function, such as the BPR (Bureau of Public Roads) function, is then used to capture the speed reduction on congested roads.

The recovery process is analyzed over a discretized period. Considering T_{max} the total time required to fully recover the system functionality under the most severe scenario, the analysis is done for each $t \in \mathcal{T}$. Thus, $T_{max} = |\mathcal{T}| \times \Delta t$, with $|\mathcal{T}|$ being the number of discrete time intervals and Δt the time unit represented by each time interval (e.g., day).

Safety: As in [33], the safety target aims to ensure that users are shielded from potential hazards, i.e., that roads are safe after the occurrence of a disruptive event. The recovery stage requires that the safety index determine the safe and unsafe roads at the time step t, according to the recovery rate ρ and the recovery priority. The safety index can be represented as the following Eq. (1).

$$S_{i,l,t} = \begin{cases} 1\ (safe) & A_{i,l,t} = 1 \\ 0\ (unsafe) & A_{i,l,t} < 1 \end{cases} \qquad \forall i \in \mathcal{N}, \forall l \in \mathcal{L}, \forall t \in \mathcal{T} \tag{1}$$

Table 2
Equations for targets extended to the time domain, adapted from [33].

Target	At OD level $\forall pq \in \mathcal{PQ}, \quad \forall l \in \mathcal{L}, \quad \forall t \in \mathcal{T}$	At the system level $\forall l \in \mathcal{L}, \quad \forall t \in \mathcal{T}$
Connectivity (C)	$C_{pq,l,t} = \begin{cases} 0 & if\ \mathcal{R}_{pq,l,t} = \emptyset \\ 1 & if\ \mathcal{R}_{pq,l,t} \neq \emptyset \end{cases}$	$C_{l,t} = \frac{\sum_{pq \in \mathcal{PQ}} C_{pq,l,t}}{\sum_{pq \in \mathcal{PQ}} \lvert\mathcal{R}_{pq,0}\rvert}$
Reliability (RL)	$RL_{pq,l,t} = \frac{\min_{r \in \mathcal{R}_{pq,0}} \{\tau_r\}}{\min_{r \in \mathcal{R}_{pq,l}} \{\tau_{r,t}\}}$	$RL_{l,t} = \frac{1}{\lvert\mathcal{PQ}\rvert} \sum_{pq \in \mathcal{PQ}} R_{pq,l,t}$
Efficiency (E)	$E_{pq,l,t} = \frac{d^g_{pq}}{\lvert\mathcal{R}_{pq,l,t}\rvert} \frac{\sum_{r \in \mathcal{R}_{pq,l}} \frac{X_{r,t}}{d_{r,t}}}{\sum_{r \in \mathcal{R}_{pq,l,t}} X_{r,t}}$	$E_{l,t} = \frac{1}{\lvert\mathcal{PQ}\rvert} \sum_{pq \in \mathcal{PQ}} E_{pq,l,t}$

Notation: $\mathcal{R}_{pq,l,t}$ is the set of available routes connecting the OD pair pq under damage level l at the time step t. Sub-index 0 means normal conditions. τ_r is the travel time associated with route r. d^g_{pq} and d_r are the geometric distance and route length, respectively. X_r is the total users of route r.

where $A_{i,l,t}$ is the portion of road i that has been restored under damage level l at time step t. When $A_{i,l,t} = 1$, it implies that the road is completely available. The restoration activities are constrained by the recovery rate, as follows:

$$\sum_{i \in \mathcal{N}} \frac{(A_{i,l,t} - A_{i,l,t-1}) D_i}{\Delta t} \leq \rho_l \qquad \forall l \in \mathcal{L}, \forall t \in \mathcal{T} \tag{2}$$

where D_i refers to the length of road i. The recovery rate, ρ_l, is expressed in length per time unit and is calculated as follows;

$$\rho_l = \frac{\sum_{i \in \mathcal{N}} (1 - A_{i,l,0}) D_i}{T_l} \qquad \forall l \in \mathcal{L} \tag{3}$$

where $A_{i,l,0}$ is the percentage of road that is not affected before the restoration activities and T_l is the total recovery time required to recover the traffic network under damage level l.

Safety at a network level is assessed considering the portion of safe roads to the total number of roads in the network for each damage level at each time step, as expressed in Eq. (4).

$$S_{l,t} = \frac{1}{|\mathcal{N}|} \sum_{i \in \mathcal{N}} S_{i,l,t} \qquad \forall l \in \mathcal{L}, \forall t \in \mathcal{T} \tag{4}$$

where $|\mathcal{N}|$ refers to the total number of roads.

Other targets, such as connectivity, reliability, and efficiency, are also considered. In this case, connectivity refers to the evaluation of network mobility at any time step t. It assesses the disconnected regions and the network's redundancy, considering the number of routes in each OD pair. Reliability is assessed regarding travel time, determining if travelers can reach their destinations within the expected time under given conditions [41]. Its calculation consists of the ratio of the minimum travel time of the OD pairs under normal and disrupted conditions at the time step t. Efficiency considers the quality of service of the network in terms of demand capacity and mobility. Therefore, efficiency is measured by the proximity of the driving distance to the minimum geometric distance as well as the proportion of users associated with a route. The complete formulation of these targets is summarized in Table 2. The second column indicates the target calculation at the OD level and the third column at the network level. These equations are derived from those presented by Arango et al. [33], with the incorporation of a time dimension.

It is clarified that target values equal to 1 represent optimal performance. For example, an efficiency index close to unity indicates an

$$PM_t = \left| \begin{array}{ccc|c} & & & Performance\ at\ time\ t \\ S_{1,t} & \cdots & S_{L,t} & \rightarrow \frac{1}{|\mathcal{L}|}\sum_{l\in\mathcal{L}} S_{l,t} = \bar{S}_t \\ C_{1,t} & \cdots & C_{L,t} & \vdots \\ RL_{1,t} & \cdots & RL_{L,t} & \vdots \\ E_{1,t} & \cdots & E_{L,t} & \rightarrow \frac{1}{|\mathcal{L}|}\sum_{l\in\mathcal{L}} E_{l,t} = \bar{E}_t \end{array} \right|$$

Fig. 4. Performance Matrix for time t.

efficient network, while values near zero signify inefficiency. On the other hand, safety and connectivity are linked. When a road does not meet the safety criteria indicates that the road has not been restored and is therefore not considered as available because of the existence of potential elements impeding safe transit. Consequently, routes passing through this particular road are disabled. Similarly, reliability and efficiency are associated with connectivity.

In general, the assessment of the targets is consistent with the preparedness framework, with one notable exception, safety. When it comes to safety, the target's goal remains the same, but the methodology for calculating the safety index differs. While in the original approach, safety focuses on the fire arrival time to a road, in the recovery assessment, the emphasis shifts to the restoration of the road.

3.4. Dynamic thresholds for recovery

Dynamic thresholds define the desirable recovery performance of target $j \in \mathcal{M}$ at each damage level, $l \in \mathcal{L}$, denoted by $Threshold_{j,l,t}$ with $t = t^*$. This means that it is not only important to define the acceptable performance but also the time to reach such performance, i.e., t^*. Thus, dynamic thresholds are defined in terms of the *desired maximum time to recover a given level of functionality for each level of damage*. An example of a dynamic threshold could be, for a minor damage level, the system is expected to recover 80% of its capacity in 2 days. For a medium-high level of damage, the system is expected to recover 50% of its functionality in 10 days. An example of the dynamic threshold for a specific target could be expecting 60% recovery of safety within 3 days for a minor damage level and achieving 100% safety recovery within 30 days for a medium-severe damage level.

The definition of dynamic thresholds can be driven by a variety of social, political, and economic reasons. In this paper, user serviceability is given more importance. However, it is important to note that the definition of dynamic thresholds responds to the interests of stakeholders. Therefore, they must establish them. The definition of dynamic thresholds follows the same reasoning as the preparedness framework. However, it is necessary to also define them including the temporal dimension.

3.5. Network performance and compliance levels

The functionality performance for each damage level (i.e., Negligible to extreme) and time step are all integrated within the network performance matrix. This results in an $|\mathcal{M}| \times |\mathcal{L}| \times |\mathcal{T}|$ matrix of components $f_{j,l,t}$, where $|\mathcal{M}|$ represents the number of targets, $|\mathcal{L}|$ the number of damage levels, and $|\mathcal{T}|$ the number of time steps, as established in Eq. (5). For instance, the component $f_{1,l,t}$ corresponds to safety.

$$PM_t = [f_{j,l,t}] \qquad \forall j \in \mathcal{M}, \quad \forall l \in \mathcal{L}, \quad \forall t \in \mathcal{T} \tag{5}$$

This performance matrix illustrates the variation in performance over time for each target. The evolution of the target's performance can be obtained by averaging the results across all the damage levels. Fig. 4 shows a generic performance matrix, PM_t.

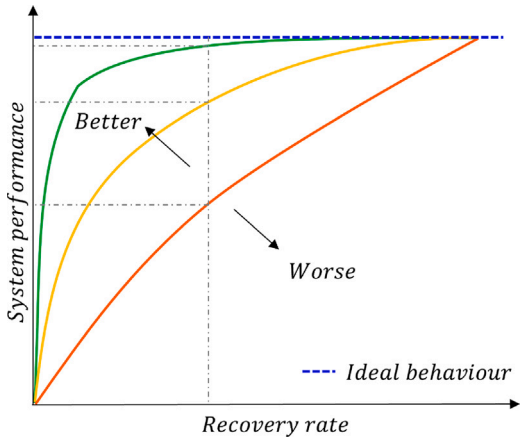

Fig. 5. Exemplification of characteristic curves depicting the system's recovery capacity, comparison of three networks.

Note that, while the intensity of the damage, ranging from negligible to extreme (i.e., the amount of obstructions), is used to estimate the recovery time, specific considerations regarding the road susceptibility are introduced limiting some unlikely damage scenarios.

On the other hand, comparing the performance with the dynamic thresholds provides the compliance values. Each compliance value, $g_{j,l} = \{0, 1\}$ indicates if the system performance fulfills the dynamic threshold associated with a given target j and damage level l at $t = t^*$. Compliance values are binary, taking either 0 or 1, where 1 indicates threshold compliance, as determined in Eq. (6).

$$g_{j,l} = \begin{cases} 0 & if\ f_{j,l,t} < threshold_{j,l,t} \\ 1 & if\ f_{j,l,t} \geq threshold_{j,l,t} \end{cases} \qquad \forall j \in \mathcal{M}, l \in \mathcal{L}, t = t^* \tag{6}$$

3.6. Characteristic curves of the system's recovery capacity

The proposed approach enables the construction of recovery characteristic curves for the traffic network. Characteristic curves describe the resilience of a system in the post-wildfire recovery phase based on the system state before the recovery process starts. Resilience is inherent to each network and depends on its ability to withstand hazardous events, influenced by the degree of system preparedness and capacity to recover. Each network possesses unique characteristics, resulting in a distinct level of preparedness and response, leading to varied recovery performances based on the degree of damage. Therefore, each network has an associated recovery capacity that, ideally, could be captured by a characteristic curve.

To illustrate the concept of the characteristic curve, three networks can be considered, each characterized by its level of preparedness, response, and recovery resources, leading to distinct recovery rates, as depicted in Fig. 5. The networks' curves are represented by green, yellow, and orange. The orange curve indicates the network with the lowest preparedness and response level resulting in more critical damage under a wildfire event. The criticality of damage experienced by a network depends on the damage distribution concerning the relevance of the affected roads and their topology. For instance, if a road network suffers damage that is concentrated on secondary roads, it may recover more easily than a network where damage is mainly concentrated on primary routes. Similarly, if the damage is concentrated in areas with greater redundancy, the network performance will be recovered much faster. It can also be observed that for a given recovery rate (e.g., dashed vertical line in Fig. 5), the recovered performance is higher for the most resilient network (the green curve).

The ideal recovery behavior would be to reach the maximum performance value even with the lowest recovery rate. This is represented by the dashed blue line in Fig. 5. The more the curve deviates from

$$S_{l,t} = \left| \begin{array}{ccc|c} S_{1,1} & \cdots & S_{1,T} & \rightarrow \quad \frac{1}{T}\sum_{t=1}^{T} S_{1,t} = S_1 \\ \vdots & \ddots & \vdots & \vdots \\ S_{L,1} & \cdots & S_{L,T} & \rightarrow \quad \frac{1}{T}\sum_{t=1}^{T} S_{L,t} = S_L \end{array} \right.$$

Fig. 6. Safety performance for different damage levels averaged over time.

the ideal recovery behavior, the worse its resilience. In other words, a greater deviation of the characteristic curve from ideal behavior indicates a lower preparedness and response level of the network and more critical damage suffered by the system.

This curve can be constructed for each target j. For the sake of clarity, the construction of the characteristic curve for the first target ($j = 1$), which is safety (i.e., $f_{j=1,l,t} = S_{l,t}$) is explained. The characteristic curve associated with safety is denoted by $\{S_l(x_l^0), \rho_l(x_l^0)\}$ with x_l^0 being the state of the system before the recovery starts. The characteristic curve is obtained by mapping the values of the safety performance matrix averaged regarding time, as shown in Fig. 6, and the associated recovery rate.

Note that the recovery rate, ρ_l, is given by the available resources and damage level, l. In contrast, the initial system state, x_l^0, depends on the damage level, which is in turn defined by the system's susceptibility and damage severity. In this sense, susceptibility is an indicator of how the system may be adversely affected by external factors or disturbances. It depends on the inherent characteristics of the system, which may make it more or less prone to critical damage or disturbance, and on its degree of risk exposure. Meanwhile, the damage severity refers to the intensity of the damage or disruption.

The information provided by the characteristic curves holds significant relevance for decision-makers, as they allow for assessing whether the available resources are adequate to address a particular level of damage. It provides insights into the attainable level of resilience during the recovery phase for different damage scenarios, highlighting the need for proactive measures to enhance the network's preparedness resilience. Essentially, it offers insights into how effectively the system responds and the extent of damage it sustains. Systems with greater resilience during the response phase tend to have more optimal curves, while less resilient systems have less optimal ones. The following section will exemplify the characteristic curves in their application to the case study.

The characteristic curves capture the system's recovery capacity under various hazard intensities and resource levels, reflecting the system in its current state. If changes are introduced, such as adding a new road or modifying vegetation, the curve will adapt, reflecting the altered recovery response of the new system. By encompassing a range of hazard and resource scenarios, the characteristic curve provides a more powerful tool for comparing systems and assessing the effectiveness of interventions than comparisons based on specific recovery scenarios.

4. Application to a case study: Pedrógão Grande, Portugal

This section presents the application of the proposed framework to assess the recovery capacity of a transportation network in a case study in Portugal, considering various levels of damage caused by wildfires. The choice of this Portuguese case study comes from the significant impact it experienced in 2017 due to severe wildfires, resulting in damages exceeding 1.5 €billion [42]. Among the affected areas was the municipality of Pedrógão Grande, situated in the Leiria district, as shown in Fig. 7. This region is predominantly covered by forests consisting mainly of pine and eucalyptus plantations. The local population consists of small towns, villages, and scattered houses, and due to the lack of adequate fuel management strategies, controlling wildfires in this area posed significant challenges. Transportation infrastructure in the study area includes important national and complementary roads, such as N2 and IC8, which support the national highway network. Consequently, this traffic network experiences high levels of activity and is important to both the region and the country.

4.1. Damage susceptibility

Due to the forested nature of the study area, damage assessment is based on the susceptibility of hazardous trees and power lines. To achieve this, an analysis of trees located near the road network was conducted, focusing on trees that could obstruct roads following a wildfire. Geographic data related to land use and occupation in the area, obtained from available Open Data at DGT [43], was utilized for this purpose. Tree species with a high capacity to spread fire and burn faster are considered, i.e., Eucalypt plantations, Maritime pine (plantations), Stone pine (plantations), and cork oaks (see classification in Fig. 8). The first two are the ones that burn the fastest and are particularly abundant in the study area.

A susceptibility zone of 7.5 m on each side of the roads was considered. This width corresponds to the average height of trees in the study area, as sourced from the forensic report [44]. That means, if a tree is less than 7.5 m from a road, it may be hazardous. In this way, the number of km of roads that would be affected in the event of hazard trees is obtained. The above is represented in Fig. 8, which shows the hazard tree susceptibility in the case study.

A total of 7 roads are not susceptible to hazard trees, such as roads 37 and 38, see cyan circle Fig. 8(a). Meanwhile, 32% of the roads are susceptible to hazard trees in their total length, e.g., roads 1 and 2 (see Fig. 8(b). The susceptibility of power poles and lines was checked on each road using Google Maps.

Once the damage susceptibility in the area has been analyzed, the different levels of damage can be estimated. For this, it is necessary to set the damage severity, which is established according to Table 3, assuming the number of downed trees and power poles per km of road. Fallen trees assumption is centered around Highway 126 in Oregon, following the severe Holiday Farm Fire, which resulted in approximately 200 hazard trees per kilometer [45,46]. For the largest damage level, a value of 100 hazard trees per kilometer is assumed, considering the area is not entirely forested, unlike the Oregon case. The values for other damage levels are extrapolated from this assumption. Meanwhile, the number of power poles is assumed having the example of the recent extreme fires on Maui (August 2023), in which more than 30 power poles came down along Honoapiilani Highway at the south end of Lahaina, causing the closure of the only route out of Lahaina to the south [47]. Five downed power poles per kilometer are assumed as the highest level of damage, based on evidence of wooden poles in the area, which was observed by walking the case study roads using Google Maps Street View. The number of power poles for the other damage levels has been extrapolated from this value. Exact values can be obtained through drones and on-site inspections, or approximate values can be obtained by consulting expert opinions.

Damage severity is expressed as the number of trees that could fall on one susceptible km of the network, which relates to the damage level. Thus, damage severity is given in terms of the number of trees and power poles that could obstruct each road of the network for each damage level, as shown in Table 3. Combining the damage susceptibility and severity for each damage level provides the number of trees and power poles fallen on each road, which must be removed during the recovery process.

It is worth mentioning that other factors, such as smoke from fires and damage to signage and guardrails, can also pose safety risks for users. These factors primarily affect visibility and traffic speed, influencing road connectivity and reliability. They have not been included in this case study. Nevertheless, the framework does allow for their consideration by including these factors in the respective targets.

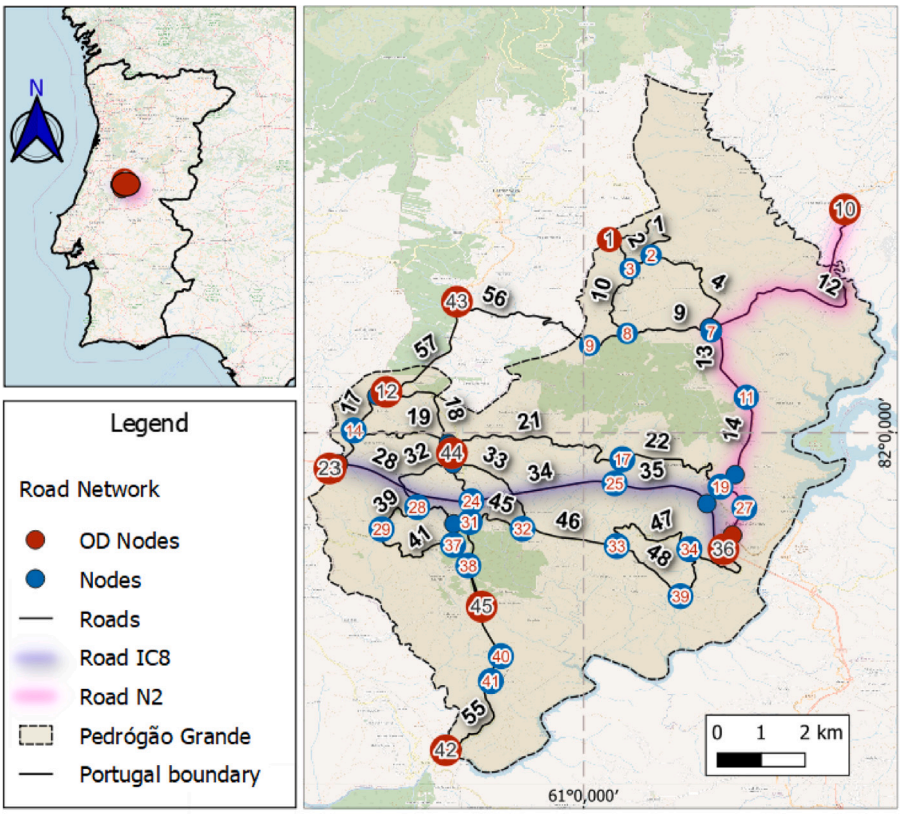

Fig. 7. Portugal Case study - Pedrógão Grande traffic network, defined by nodes and roads. Source of background: Open Street Maps.

Table 3
Damage severity associated with each damage level, in terms of hazard trees and falling power poles.

Damage level[a]	1	2	3	4	5	6	7
Trees/km	–	1	3	10	30	50	100
Power poles/km	–	–	–	1	2	3	5

[a] The numbers correspond to the different categories of damages, e.g., 1 is Negligible, 2 is Minor, and 7 is Extreme.

4.2. Traffic network information

The traffic network information consists of node coordinates, unidirectional roads, road lengths, road free-flow speeds, road flow, and road typology data. This information was provided by *Infraestruturas de Portugal S.A.*. Information about the demand associated with each OD (origin–destination) pair and the set of routes connecting each OD pair is also required. The Pedrógão Grande network comprises 118 roads and 45 nodes (see Fig. 7), with a total of 25 OD pairs considered. Detailed information about the OD pairs can be found in Table A.1 in Appendix. Regarding the traffic model parameters, they are assumed as $\alpha = 0.26$, $\beta = 1$, $\gamma = 8.4$ and $\theta = 1.2$. α, β, and γ are the BPR parameters, while θ is a parameter of the C-logit Stochastic User Equilibrium model related to the network dispersion. For detailed information on the traffic model see [39].

4.3. Criticality of the network's components

The criticality of the different components of the network is determined by analyzing how the degradation of these components impacts the overall travel time experienced by network users. Degradation refers to the gradual reduction or complete closure of individual roads. This analysis uses a traffic assignment model, operating on the principle that traffic flows through the network in a way that drivers seek to minimize their travel time. As a road's travel time depends on the congestion level, this analysis necessitates network-level optimization. Consequently, this assessment considers the topological characteristics of the road network to evaluate its connectivity, taking into account both traffic demand and network performance concerning travel time. The annual average daily traffic (AADT) assesses how a wildfire event might impact the network's capacity to handle standard traffic conditions. For a more detailed explanation of this criticality assessment, see [39].

The criticality analysis leads to the results in Fig. 9. The figure represents the criticality of each road in the Pedrógão Grande traffic network.

There are 13 roads classified with high criticality (between 0.8 and 1), within which we can find roads 34, 27, 57, 13, and 14 mainly due to the number of users and the absence of alternative routes. Examples of less critical roads are roads 49, 50, 58, and 59. The criticality ranking, which determines the importance of each road within the network, is later used to establish the order of priority for recovery activities. In other words, the most important roads will be recovered first. Other criticality analyses can be used in the methodology as long as they provide a priority ranking for recovery.

4.4. Available resources for recovery

For the quantification of the resources available in this case, the number of crews available in the area for tree and power pole removal is considered. In Portugal, rehabilitation and restoration activities are conducted by local, governmental, and private entities, mainly executed by the Firefighter Corps and, in some cases, the National Guard [48,49]. According to the Portugal Contemporaneo database, there are 45 active firefighters in the municipality of Pedrógão Grande [50]. They are normally organized in crews of 5 firefighters [51]. This gives a total of 9 crews for this area. Note that only the resources within the study area are considered. Depending on

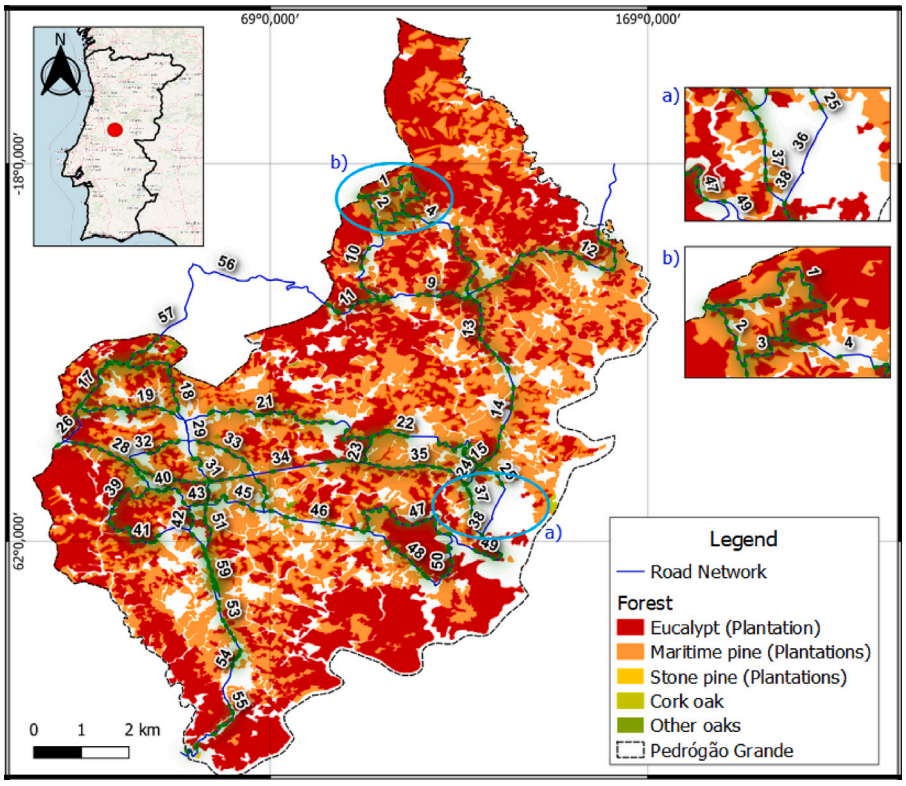

Fig. 8. Hazard trees susceptibility for Pedrógão Grande traffic network.

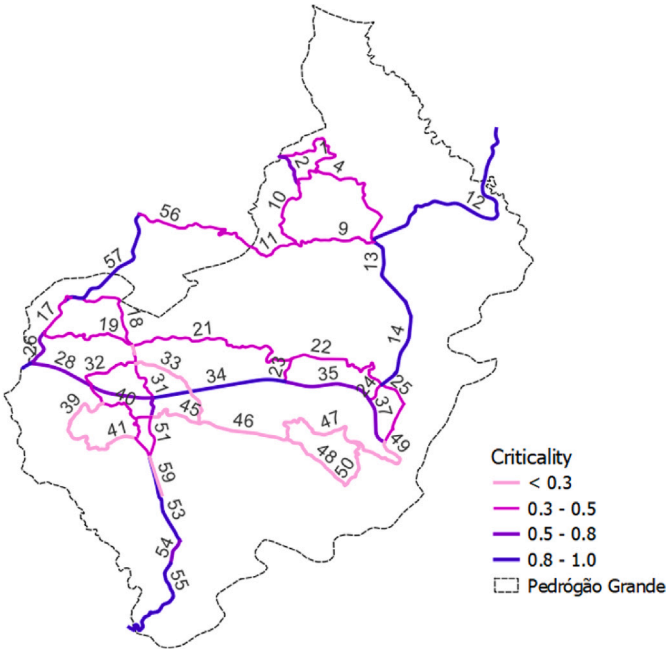

Fig. 9. Ranking of critical roads for the Pedrógão Grande traffic network.

Table 4
Tree removal times.

ID	Data	Ref	Removal time (h)
Fallen tree	A large tree (pine) fell on the roadway. The warning was given at 14.19 and the road was clear of traffic at 15.50. (2022-04-04)	[52]	1.50
Fallen tree caused fatalities	The tree hit a motorcycle and a pickup, killing both drivers. California Highway Patrol and fire crews responded to the scene around 6 a.m. One lane of traffic reopened around 8:15 a.m., so traffic slowly began to move again.	[53]	2.15
Power pole fall	Traffic was cut off from 18:50. Traffic on the avenue was re-established at 21:54	[54]	3.00

the specific circumstances, external resources can also be taken into account. For instance, additional firefighting crews from neighboring regions, departmental, or national levels, as well as crews from the Armed Forces and Republican National Guard, can be considered. It is also assumed that the crews work 10-hour workdays.

4.5. Work efficiency

Recovery times for fallen trees and power pole removal are considered as given in Table 4, these values are taken from available reports. This recovery times can serve as a base for other application cases. However, it is crucial to assess and revise them following the specific conditions of each case study.

In addition to these removal times, it is important to account for the crews' travel time. For instance, in the case of Canada, where the roads are longer, crew arrival times can exceed one hour. Removing one tree would take about 1.5 h, plus the crews' travel time. Nevertheless, for the current case study, the roads are relatively short and approximately 15 min away from the fire station, where the restoration activities are assumed to be coordinated; this additional time is not considered.

4.6. Recovery time and recovery rates calculation

For each damage level, the number of trees and power poles down on each road is calculated as explained in Section 4.1. The assumed removal time given in Section 4.5 indicates the required time for a crew to remove elements fallen on the road. The order in which the roads will be recovered is given by their criticality as explained in Section 4.3. Consequently, at each step, the number of roads recovered under different damage levels can be determined considering the available resources indicated in Section 4.4. The calculation of the total recovery time required to remove all the fallen elements associated with each level, T_l, is straightforward. Table A.2 in Appendix presents the recovery time, in days, of the entire system (i.e., complete removal of fallen trees and poles) for each road and damage level, employing 9 crews. Note that the estimated total recovery time under the most severe scenario is used to establish the time window to be analyzed, that is, $T_{max} = T_L$.

Based on the previous information, the recovery rate associated with each intensity level, ρ_l, can be calculated using Eq. (3). In this case, the recovery rate is expressed as kilometers recovered per day. Finally, the evolution of the performance of the different targets at a system level can be calculated using Eq. (4) and the expressions given in Table 2.

4.7. Dynamic thresholds

Resilience exhibits a temporal dimension. In the case of a community being cut off, the primary objective is to restore the power supply. The road, in this scenario, only needs to be partially functional, ensuring, for instance, 50% safety, i.e., allowing a few vehicles to deliver essential supplies or facilitate evacuation. Subsequently, the focus shifts to recovering connectivity, followed by reliability and, finally, efficiency. For instance, for moderate damage, the goal is to restore 50% of the safety within 3 days, 50% of the connectivity within 5 days; and achieve 90% reliability and efficiency within 30 days. The latter two requirements indicate the need for nearly complete system recovery within a month. Accordingly, it is assumed that after consultation with the stakeholders involved and interested in the road network recovery, the selected dynamic thresholds are 3, 4, 5, 6, 10, 15, and 30 days to recover 50% of safety functionality associated with damage levels negligible, minor, moderate, medium, medium to severe, severe, and extremely severe, respectively. That is,

$$Threshold_{1,l,t} = 0.5;$$
$$(l,t) = \{(1,3),(2,4),(3,5),(4,6),(5,10),(6,15),(7,30)\}$$

For the case of connectivity, the assumed thresholds are

$$Threshold_{2,l,t} = 0.5;$$
$$(l,t) = \{(1,5),(2,7),(3,9),(4,10),(5,12),(6,20),(7,45)\}$$

and for the case of reliability and efficiency, the thresholds are

$$Threshold_{\{3,4\},l,t} = 0.9;$$
$$(l,t) = \{(1,15),(2,21),(3,30),(4,90),(5,180),(6,365),(7,500)\}$$

4.8. Results

According to the initial damage established with the susceptibility of hazard trees and power poles, Fig. 10 shows the total recovery time for the traffic network as a function of the number of available crews and damage levels resulting from the fire suppression. As expected, increasing the number of crews reduces the total recovery time for all damage levels, with the most significant difference observed between medium and extreme damage levels. For instance, for extreme damage, the recovery time of the system with 1 crew is 7 times higher than having 9 crews. In this case, relying on a single crew might not be acceptable because the recovery process will take around two years. These recovery times can take several months to complete, e.g., in the case of Oregon, the recovery process took about 18 months [55]. Decision-makers should consider the trade-off between the cost of adding resources (crews) and the societal consequences associated with a prolonged recovery process.

More detailed information about the network recovery is obtained by plotting the performance associated with each target at different damage levels over time. See Fig. 11. These curves represent the response of the system when all available crews are engaged in recovery efforts. In this sense, Fig. 11 illustrates the recovery profile of the safety and connectivity targets for each initial damage level. At the negligible level, where no damage is implied, safety remains intact since there are no unsafe roads for users. As the damage level increases, the recovery curves become less steep, indicating a more extended time required for recovery. Up to the medium damage level, safety is fully restored in less than 10 days, while at medium to extreme damage levels, it takes 30 to 80 days for safety to recover. However, what determines whether the recovery performance is enough is the comparison with the dynamic thresholds. The thresholds are represented with an asterisk. Safety performance meets the accepted threshold for the first four damage levels, that is, 50% of functionality associated with damage levels negligible, to medium is obtained before 3, 4, 5, and 6 days. However, for medium-severe to extreme damage levels, the accepted performance is not achieved, with the curves falling to the right of the dynamic threshold. The black arrows indicate the difference between actual safety performance and the thresholds. For example, in the most critical case of extreme damage, the target is to restore 50% of network safety within 30 days but the actual safety recovered at this time is only 31%. In contrast, the 45-day threshold is sufficient to recover 50% of connectivity; in fact, at this time connectivity is over 70%.

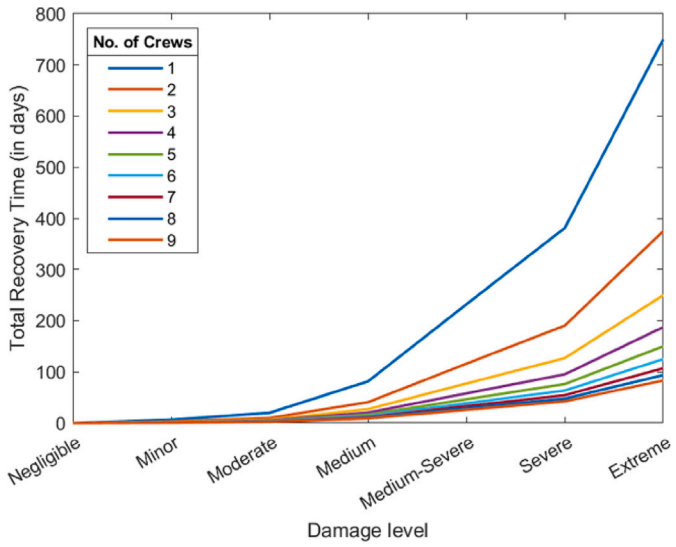

Fig. 10. Total recovery time according to each damage level resulting after the fire suppression and number of crews available.

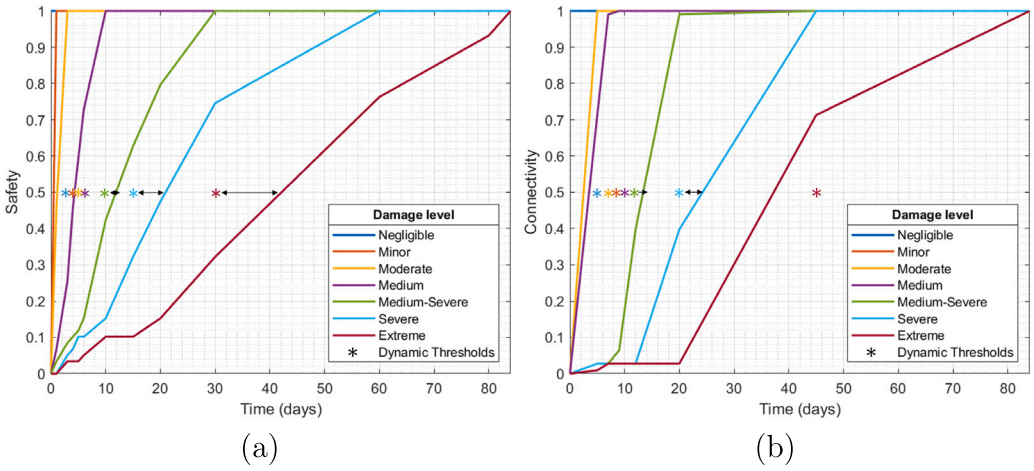

Fig. 11. Recovery profile of (a) safety and (b) connectivity associated with different damage levels. 9 crews considered.

It is evident the hierarchy between the targets, where connectivity depends on safety. For instance, 10 days after a medium-severe damage event (green curve), more than 40% of safety has been recovered, while connectivity has reached less than 20%. Besides, after a period of little recovery of the connectivity, the recovery curves for connectivity exhibit steeper slopes than the safety curves for all damage categories. This is due to the need to open critical road segments before different OD pairs are reconnected again.

On the other hand, Fig. 12 offers a comprehensive view of safety performance during the recovery stage concerning varying resource units, i.e., the number of crews available. This graph consolidates the information from the previously presented results for all possible crew combinations by following the process outlined in Fig. 6, logging safety performance values at each evaluated time step and damage level. Subsequently, each point represents the average safety performance achieved by the corresponding number of crews during the considered time steps. For instance, when only one crew is available for recovery activities following a moderate level of damage, network safety remains above 50% throughout the recovery time window. In this way, it is possible to determine the number of crews required for a specific safety performance. For example, to ensure an 80% safety level for a minor damage state during the recovery time, one crew would suffice. However, for a moderate damage level, at least 3 crews would be needed at the same safety level. For the other damage levels, that safety level could not be ensured with the currently available resources.

Another insightful way to represent the results is the performance of a target as a function of the recovery rate. This is exemplified by focusing on the safety target when considering the 9 crews. For this, the formulation of the characteristic curve, Section 3.6, is followed. Fig. 13 represents the average safety performance (throughout the recovery time step) as a function of the recovery rate.

The obtained results provide valuable insights, reflecting the information shown in Fig. 12. For instance, for minor levels of damage, safety remains consistently high throughout the recovery time window. This indicates that the recovery rate, given the available resources, effectively restores safety performance promptly after a disruptive event. However, for medium-severe damage levels, the average safety value drops to less than 55% during the recovery time. This suggests that even with the maximum recovery resources (i.e., 9 crews), it takes longer to restore network safety at this damage level.

The discussed curve represents safety performance with a specific resource allocation, i.e., 9 crews. Nonetheless, examining all possible combinations of available resources (crews) leads to a complete characteristic curve of the system recovery, as shown in Fig. 14. This characteristic curve illustrates safety recovery capacity regarding achievable recovery rates based on resource availability. It offers more complete

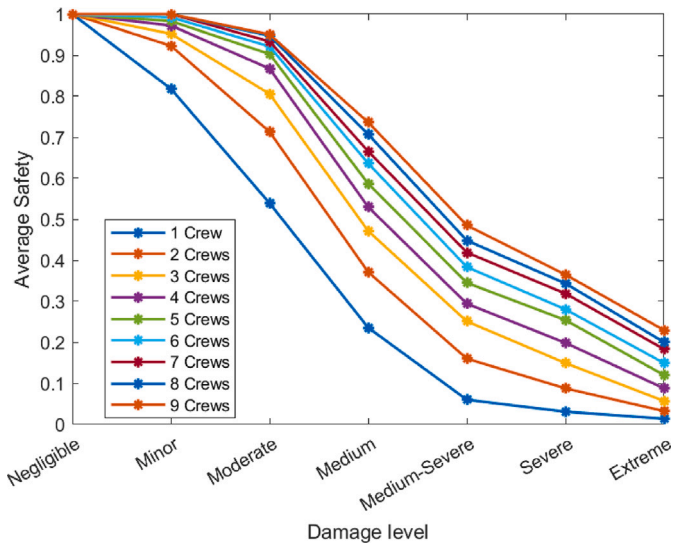

Fig. 12. Average safety performance of the Pedrógão Grande Traffic network for different numbers of crews and levels of damage.

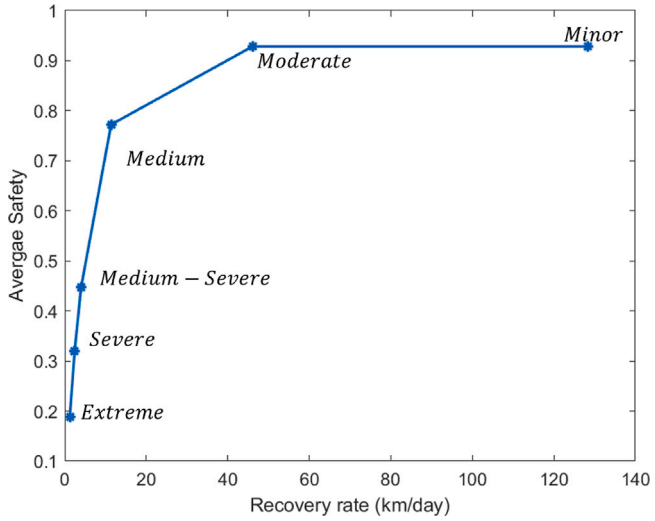

Fig. 13. Average safety target through the time steps associated with 9 crews. Construction step of the characteristic curve for safety recovery capacity.

information than the previous curves (e.g., Figs. 12 and 13), as it condenses the safety performance and the recovery rate for each damage level and amount of resources. Thus, it is possible to observe that at a minor damage level, 100% safety can be assured with 7 crews or more. The recovery rate achieved by this number of crews is sufficient to maintain that level of safety. In contrast, the recovery rate achieved by a single crew is 9 times lower, and therefore, it only guarantees 80% network safety. As damage severity increases, the recovery rate decreases, leading to reduced network safety. Consequently, with the available resources, ensuring network safety becomes challenging for moderate to high damage levels.

These curves are intrinsic to the network. The behavior of the curve depends on the damage susceptibility (which relates to roads prone to obstructions from hazard trees and power poles), however, the curve's tendency is independent of the assumed damage severity (which relates to the percentage of trees and poles falling due to different fire intensities), i.e., the number of hazard trees and power poles. To illustrate this, two scenarios of damage severity are compared within the same case study, (i) the reference case with the current damage severity and (ii) an alternative case with 10 times the current damage severity. In both scenarios, the damage susceptibility remains the same for the network. Still, the assumed damage severity for each damage level is increased by a factor of 10, i.e., 10 times the values in Table 3. Fig. 15 shows that the curve follows the same trend for both scenarios, albeit, within different ranges, i.e., both curves overlap and describe the same behavior. In this sense, the damage susceptibility is responsible for the shape of the curve and damage severity defines the position within the curve. Therefore, the trend exhibited by the characteristic curves will be the same regardless of the damage levels, susceptibility and severity, and available resources, because the curve represents the intrinsic recovery capacity of the system under different circumstances. The characteristic curves of connectivity and reliability are shown in Appendix, in Figs. A.1 and A.2.

4.9. Discussion of results

The proposed framework provides relevant information to stakeholders regarding the system's recovery time based on available resources and the level of damage incurred. This offers a more comprehensive perspective on the system's behavior and whether available resources are enough for an acceptable recovery, i.e., thresholds. For instance, in the case study, if only 3 crews were available, the total recovery time for severe and extreme damage levels would be three

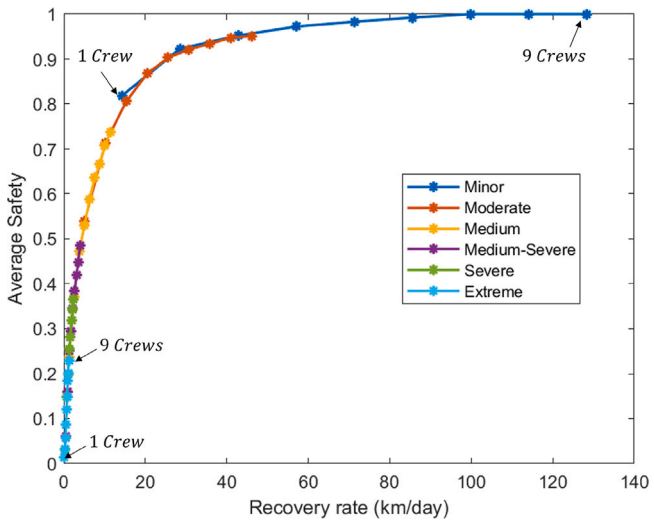

Fig. 14. Characteristic curve of safety recovery capacity for the Pedrógão Grande traffic network, Portugal. Average Safety through the time step.

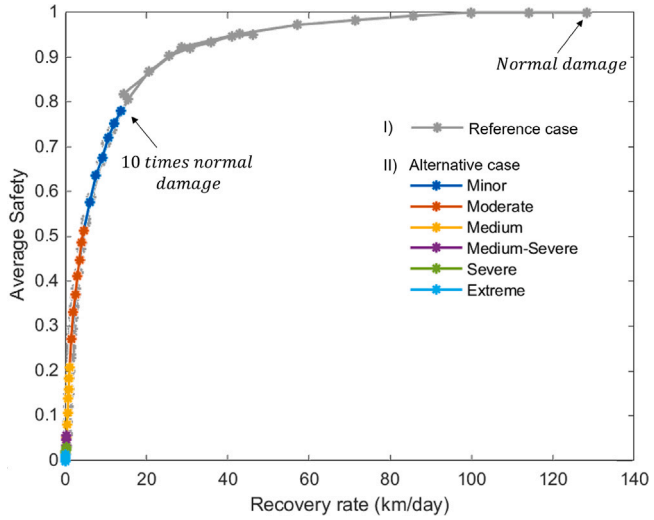

Fig. 15. Influence of different initial damage state in the characteristic curve of the recovery capacity of safety for the Pedrógão Grande traffic network, Portugal.

times longer, resulting in a total of 251 days. Therefore, the framework also allows comparison between networks and different conditions.

Another relevant information for stakeholders is comparing network recovery performance based on thresholds and available resources. Considering the case of safety performance, that comparison is present in Fig. 16, which represents the relationship between the damage levels and recovery rates in terms of kilometers recovered per day. It shows that at high damage levels, the recovery rates are not compliant, even when maximum resources are available. That is, for damage levels ranging from medium-severe to extreme, the kilometers recovered per day are insufficient to achieve the expected recovery. This suggests that the municipality's resources would not be sufficient to handle such levels of damage, and therefore, actions are necessary. In addition, a single crew would not be sufficient to recover the required kilometers for the damage levels above minor.

Informed decisions about the allocation of resources concerning the extent of damage are essential. Therefore, the system's characteristic curves could be an important tool to support decision-making. Using the example of the safety recovery characteristic curve in Fig. 14, the stakeholders can determine the necessary resources to ensure a specific safety level for a particular damage level. For instance, 90% of safety can be guaranteed either with 2 crews for minor damage or with 4 crews for a moderate damage level. However, for the other damage levels, the resources are not enough to guarantee this safety level for the network. The stakeholders should reflect on the desired safety level during the recovery time. Accordingly, the proposed curves can inform whether the internal resources are sufficient to achieve this or whether different actions are needed.

Those actions can be reactive, to improve the recovery rates, or proactive, to increase resilience in terms of preparedness and minimize the system damage impact by possible events. One of the reactive measures that can be taken is utilizing external resources. When dealing with extreme wildfires, external assistance usually plays a central role in supporting affected communities during recovery. Assistance from agencies or organizations at various levels (such as local, state, and federal) can offer aid within different time frames. In this case, the resources required to fulfill the accepted recovery times are more than 13 crews. The additional resources improve recovery rates and, therefore, network performance restoration times.

If external crews are unavailable, the response conditions can be enhanced by increasing the level of preparedness resilience. In other

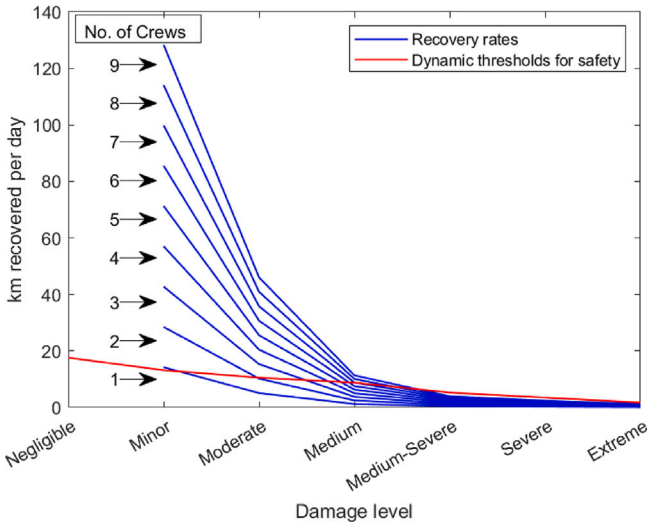

Fig. 16. Compliance of recovery rates with dynamic thresholds in the case of safety.

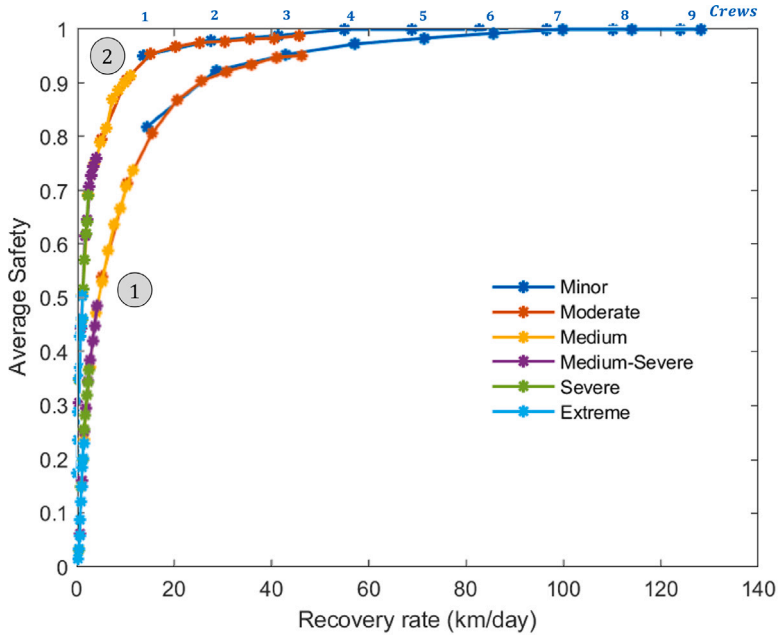

Fig. 17. Characteristic curve of safety recovery capacity for the Pedrógão Grande traffic network. (1) Reference case. (2) Introducing vegetation management policies.

words, adjustments should be made in earlier stages through adaptation. In this context, considering the framework's assessment of damage susceptibility, it is possible to analyze the most exposed areas within the network. This analysis allows the implementation of proactive measures to mitigate potential fire damage before an event occurs. These measures may include vegetation management, e.g., the creation of firebreaks, and the reinforcement of power poles. For instance, if firebreaks were implemented to manage the hazard trees for half of the roads, the resilience would increase as well as the capacity to recover, as it reduces the network's susceptibility. Firebreak is understood as a series of actions related to vegetation management aimed at reducing fire exposure [56], e.g., removing the trees around the roads. The influence of this adaptation option and its influence on the resilience and recovery increase is demonstrated in Fig. 17. This figure compares the safety recovery capacity of the network of the reference case, represented by Curve 1, and an alternative case, that accounts for the introduction of firebreaks, represented by Curve 2. This, considering that firebreaks are applied to half of the most relevant roads, following the criticality ranking. Generally, better network safety performance is achieved with a lower recovery rate, moving the curve closer to the ideal behavior. Thus, 4 crews would be needed to guarantee the total safety of the network, as opposed to the present case (Curve 1) where at least 7 crews are required.

This also demonstrates that the characteristic curves allow the comparison of networks in terms of their recovery performance, highlighting that the alternative case (Curve 2) is more resilient than the reference one (Curve 1).

5. Conclusions

This work is presented as an extension of the preparedness resilience framework [33], addressing recovery assessment. Based on the preparedness framework, this framework evaluates response behavior for different levels of damage, encompasses different system functionalities, and incorporates dynamic thresholds. However, to incorporate recovery performance, the framework has added a temporal dimension,

allowing the consideration of aspects such as recovery time and recovery rate. They depend on the amount of resources available for recovery activities. Thus, the framework provides a more complete picture of system behavior during the recovery stage, as demonstrated in the application of the case study of the Pedrógão Grande traffic network.

The framework permits the generation of the recovery characteristic curves of the system. They capture the recovery capacity of a network, consider the system preparedness capacity, and include relevant information for the analysis of the recovery stage. It can be very useful for classifying and analyzing network resilience in terms of recovery, thus avoiding a detailed analysis of many scenarios and the assumptions they entail. As these curves are intrinsic to each network, they enable network comparisons. Thus resolving the limitations found in the scientific literature frameworks. This paper has proposed some representations of recovery assessment. However, the characteristic curves aggregate the meaningful information of those representations into a single curve, allowing for the comparison of the impacts of different wildfire management decisions. Alternative representations of the studied dimensions, including 3D models, could also be considered. Additionally, since the approach supports the analysis of various decisions, it could be extended into a prescriptive tool, which will be explored in future studies.

This framework offers several advantages over others in the analysis of recovery; (i) It avoids dependence on specific scenarios by considering the susceptibility of damage across the entire network, instead of assuming damage in specific roads. It also accounts for various levels of damage, providing insights into network behavior across a damage range. The creation of characteristic curves of the system recovery also reinforces this advantage of being scenario-free oriented, since the characteristic curves are independent of the damage scenarios; (ii) It provides an overview of the system's recovery capacity by evaluating different functionalities, including safety, connectivity, and reliability. In addition, it eliminates the need to study all possible damage scenarios to make informed decisions about system recovery. This can mean a significant reduction in computational cost; (iii) It aids in understanding and decision-making regarding resource availability for recovery activities, as it evaluates system performance for all possible resource combinations. Thus, stakeholders can determine what amount of resources are needed to obtain a certain performance, that complies with the required acceptable behavior; (iv) The framework enables an assessment of the adequacy of a system's resilience to withstand damage, determining whether the available resources are sufficient for recovery or if additional actions are necessary, i.e., external resources or achieving the required resilience during the preparedness stage.

The framework has some limitations, such as the assumption of damage severity and criticality assessment. Damage severity may be overestimated because the data are based on records of fire consequences in another country. However, by considering different levels of damage, the analysis provides more information and is more conservative. Furthermore, this limitation can be addressed with the use of expert judgment, drones, and inspections during a real event. Regarding criticality consideration, it may not be realistic to evaluate each road separately; ideally, criticality should be discriminated by routes. This aspect will be addressed in future studies. While originally used for traffic networks and wildfires, this approach can be extended to different systems such as power transmission networks, as well as to various types of hazards by establishing suitable targets, levels of damage, and dynamic criteria.

CRediT authorship contribution statement

Erica Arango: Writing – review & editing, Writing – original draft, Visualization, Validation, Supervision, Methodology, Investigation, Funding acquisition, Formal analysis, Data curation, Conceptualization. **Maria Nogal:** Writing – review & editing, Writing – original draft, Validation, Supervision, Methodology, Investigation, Formal analysis, Conceptualization. **Ming Yang:** Writing – review & editing, Supervision, Methodology, Conceptualization. **Hélder S. Sousa:** Writing – review & editing, Supervision, Funding acquisition. **José C. Matos:** Writing – review & editing, Supervision, Funding acquisition. **Mark G. Stewart:** Writing – review & editing, Validation, Supervision, Methodology.

Declaration of competing interest

The authors declare the following financial interests/personal relationships which may be considered as potential competing interests: Erica Arango reports financial support was provided by Foundation for Science and Technology. If there are other authors, they declare that they have no known competing financial interests or personal relationships that could have appeared to influence the work reported in this paper.

Acknowledgments and funding statement

This work was partly financed by FCT/MCTES, Portugal through national funds (PIDDAC) under the R&D Unit Institute for Sustainability and Innovation in Structural Engineering (ISISE), under reference UIDB/04029/2020 (doi.org/10.54499/UIDB/04029/2020), and under the Associate Laboratory Advanced Production and Intelligent Systems ARISE, Portugal under reference LA /P /0112/2020.

This work is financed by national funds through the FCT, Foundation for Science and Technology, Portugal, under grant agreement 2020.05755.BD (doi.org/10.54499/2020.05755.BD) attributed to the first author.

This work was also supported by the Dutch Research Council (NWO), Netherlands and the Department of Science & Technology, India (DST), through the Merian Fund under Grant No. 482.482.302.

Appendix. Input data and results

Traffic input parameters per OD are given in Table A.1.

Table A.1
Origin–destination pair nodes, demand, and the number of routes considered for the Pedrógão Grande traffic network.

Origin node	Destination node	OD demand (users/hour)	No. of routes
1	35	390	5
1	36	438	5
10	22	251	5
10	36	290	5
10	22	250	5
12	36	550	5
12	43	653	1
22	35	370	5
22	36	1061	5
22	43	431	5
23	35	222	5
23	36	600	5
23	42	672	5
10	1	285	5
36	1	537	5
22	10	603	5
36	10	223	5
36	12	687	5
43	12	711	1
23	22	329	1
35	22	591	5
36	22	888	5
43	22	541	5
35	23	422	5
36	23	605	5

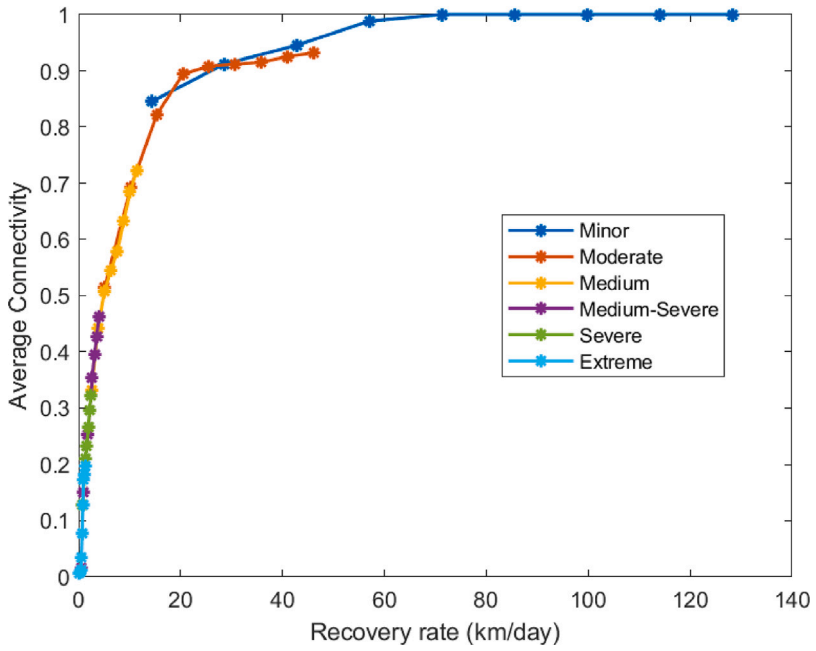

Fig. A.1. Characteristic curve of connectivity recovery capacity for the Pedrógão Grande traffic network, Portugal.

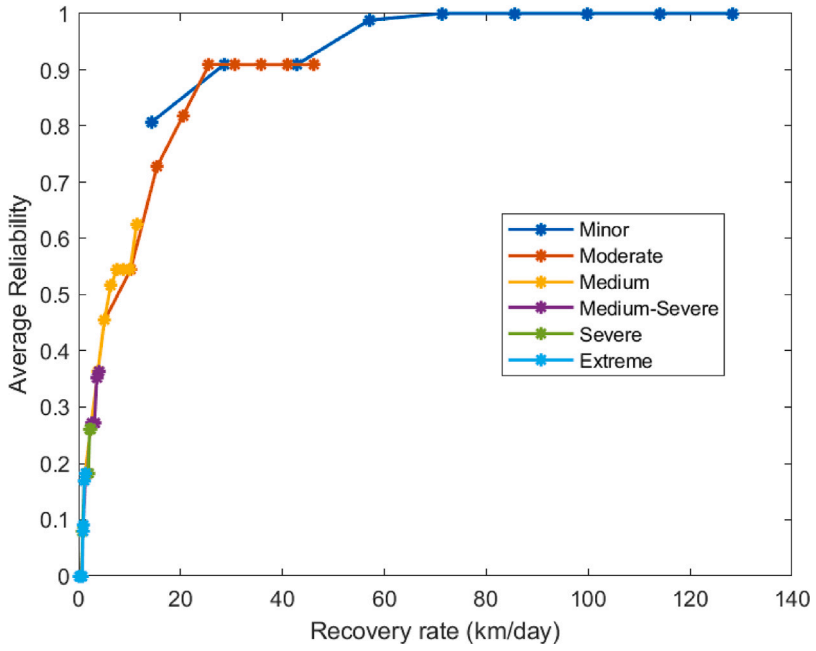

Fig. A.2. Characteristic curve of reliability recovery capacity for the Pedrógão Grande traffic network, Portugal.

Table A.2
Total recovery time in days per road (9 crews). Numbers 1, 2, ...7, correspond to the Negligible to extreme damage levels respectively.

Roads	Damage levels						
	1	2	3	4	5	6	7
1	0,00	0,03	0,11	0,46	1,28	2,13	4,12
2	0,00	0,01	0,03	0,16	0,43	0,71	1,42
3	0,00	0,01	0,03	0,10	0,31	0,51	1,03
4	0,00	0,03	0,09	0,39	1,04	1,73	3,37
5	0,00	0,00	0,00	0,00	0,00	0,00	0,00
6	0,00	0,00	0,00	0,00	0,00	0,00	0,01
7	0,00	0,00	0,00	0,00	0,00	0,00	0,00
8	0,00	0,00	0,00	0,00	0,01	0,01	0,03
9	0,00	0,02	0,06	0,26	0,68	1,13	2,24
10	0,00	0,01	0,04	0,19	0,57	0,91	1,79
11	0,00	0,01	0,03	0,14	0,41	0,67	1,31
12	0,00	0,06	0,16	0,69	1,86	3,06	5,94
13	0,00	0,02	0,07	0,22	0,66	1,09	2,17
14	0,00	0,02	0,06	0,24	0,62	1,03	2,01
15	0,00	0,00	0,01	0,06	0,17	0,28	0,54
16	0,00	0,00	0,01	0,03	0,09	0,16	0,30
17	0,00	0,01	0,03	0,16	0,44	0,73	1,47
18	0,00	0,03	0,10	0,42	1,17	1,91	3,68
19	0,00	0,02	0,07	0,29	0,80	1,31	2,56
20	0,00	0,00	0,00	0,00	0,00	0,00	0,00
21	0,00	0,04	0,12	0,53	1,44	2,38	4,63
22	0,00	0,02	0,08	0,33	0,96	1,54	3,02
23	0,00	0,01	0,02	0,08	0,24	0,41	0,82
24	0,00	0,00	0,01	0,04	0,14	0,23	0,48
25	0,00	0,00	0,01	0,04	0,18	0,27	0,53
26	0,00	0,00	0,01	0,04	0,14	0,23	0,47
27	0,00	0,00	0,00	0,01	0,03	0,06	0,10
28	0,00	0,03	0,10	0,34	1,02	1,70	3,40
29	0,00	0,00	0,00	0,00	0,00	0,00	0,00
30	0,00	0,00	0,00	0,00	0,00	0,00	0,00
31	0,00	0,01	0,02	0,09	0,21	0,36	0,69
32	0,00	0,01	0,04	0,13	0,41	0,69	1,39
33	0,00	0,02	0,07	0,30	0,82	1,34	2,62
34	0,00	0,02	0,07	0,23	0,70	1,17	2,33
35	0,00	0,02	0,08	0,26	0,76	1,26	2,52
36	0,00	0,00	0,00	0,00	0,00	0,00	0,00
37	0,00	0,01	0,02	0,09	0,26	0,43	0,87
38	0,00	0,00	0,00	0,00	0,00	0,00	0,00
39	0,00	0,01	0,04	0,18	0,54	0,87	1,70
40	0,00	0,01	0,02	0,09	0,20	0,34	0,66
41	0,00	0,02	0,07	0,29	0,80	1,30	2,54
42	0,00	0,01	0,02	0,07	0,21	0,36	0,72
43	0,00	0,00	0,01	0,04	0,16	0,23	0,48
44	0,00	0,00	0,01	0,06	0,19	0,29	0,57
45	0,00	0,01	0,02	0,12	0,34	0,52	1,04
46	0,00	0,01	0,02	0,10	0,24	0,42	0,81
47	0,00	0,03	0,11	0,36	1,07	1,77	3,54
48	0,00	0,01	0,04	0,19	0,58	0,93	1,82
49	0,00	0,02	0,06	0,23	0,61	1,02	1,98
50	0,00	0,01	0,02	0,09	0,26	0,42	0,84
51	0,00	0,01	0,03	0,12	0,37	0,61	1,23
52	0,00	0,00	0,01	0,04	0,13	0,22	0,44
53	0,00	0,01	0,04	0,20	0,59	0,94	1,86
54	0,00	0,00	0,01	0,04	0,16	0,23	0,47
55	0,00	0,01	0,03	0,14	0,39	0,64	1,24
56	0,00	0,00	0,01	0,04	0,17	0,24	0,50
57	0,00	0,01	0,04	0,18	0,54	0,88	1,72
58	0,00	0,00	0,00	0,00	0,00	0,00	0,00
59	0,00	0,01	0,03	0,14	0,41	0,67	1,30
T_l	0	1	2	9	26	42	83

References

[1] News TG. Greece wildfire declared largest ever recorded in EU. 2023, URL https://www.theguardian.com/world/2023/aug/29/greece-wildfire-declared-largest-ever-recorded-in-eu.

[2] Harmsworth E. Wildfires cost Europe € 4.1 billion as temperatures hit records. 2023, URL https://www.bloomberg.com/news/articles/2023-09-04/greece-suffers-most-damage-as-wildfires-cost-europe-4-1-billion?embedded-checkout=true.

[3] JRC. Wildfires in the mediterranean: monitoring the impact, helping the response. 2023, URL https://joint-research-centre.ec.europa.eu/jrc-news-and-updates/wildfires-mediterranean-monitoring-impact-helping-response-2023-07-28_en.

[4] News C. Hawaii probes unsolicited offers for land after fires, pledges to keep land in local hands. 2023, URL https://www.cbc.ca/news/world/hawaii-property-lahaina-wildfires-1.6954189.

[5] Rafferty JP. Maui wildfires of 2023 - natural disaster, Hawaii, United States. 2023, URL https://www.britannica.com/event/Maui-wildfires-of-2023.

[6] Hassan A, Betts A. Maui wildfires latest: Lahaina reopens to residents. 2023, URL https://www.nytimes.com/article/maui-wildfires-hawaii.html.

[7] DFFP. CAL FIRE serves and safeguards the people and protects the property and resources of California. 2023, URL https://www.fire.ca.gov/incidents.

[8] Zhou Y, Wang J, Yang H. Resilience of transportation systems: Concepts and comprehensive review. IEEE Trans Intell Transp Syst 2019;20(12):4262–76. http://dx.doi.org/10.1109/TITS.2018.2883766.

[9] YuanChi Liu JH, Adey BT. Prioritizing transportation network recovery using a resilience measure. Sustain Resilient Infrastruct 2022;7(1):70–81. http://dx.doi.org/10.1080/23789689.2019.1708180.

[10] Koc E, Cetiner B, Rose A, Soibelman L, Taciroglu E, Wei D. Comprehensive resilience assessment framework for transportation systems in urban areas. Adv Eng Inform. 2020;46:101159. http://dx.doi.org/10.1016/j.aei.2020.101159.

[11] Council NR, et al. Disaster resilience: A national imperative. Washington, DC: The National Academies Press; 2012, http://dx.doi.org/10.17226/13457, URL https://nap.nationalacademies.org/catalog/13457/disaster-resilience-a-national-imperative.

[12] Nogal M, Honfi D. Assessment of road traffic resilience assuming stochastic user behaviour. Reliab Eng Syst Saf 2019;185:72–83. http://dx.doi.org/10.1016/j.ress.2018.12.013.

[13] Zou Q, Chen S. Resilience-based recovery scheduling of transportation network in mixed traffic environment: A deep-ensemble-assisted active learning approach. Reliab Eng Syst Saf 2021;215:107800. http://dx.doi.org/10.1016/j.ress.2021.107800.

[14] Zhang M, Yang X, Zhang J, Li G. Post-earthquake resilience optimization of a rural "road-bridge" transportation network system. Reliab Eng Syst Saf 2022;225:108570. http://dx.doi.org/10.1016/j.ress.2022.108570.

[15] Pan X, Dang Y, Wang H, Hong D, Li Y, Deng H. Resilience model and recovery strategy of transportation network based on travel OD-grid analysis. Reliab Eng Syst Saf 2022;223:108483. http://dx.doi.org/10.1016/j.ress.2022.108483.

[16] Wang N, Yuen KF. Resilience assessment of waterway transportation systems: Combining system performance and recovery cost. Reliab Eng Syst Saf 2022;226:108673. http://dx.doi.org/10.1016/j.ress.2022.108673.

[17] Yang S, Zhang Y, Lu X, Guo W, Miao H. Multi-agent deep reinforcement learning based decision support model for resilient community post-hazard recovery. Reliab Eng Syst Saf 2024;242:109754. http://dx.doi.org/10.1016/j.ress.2023.109754.

[18] Lu Q-C, Li J, Xu P-C, Zhang L, Cui X. Modeling cascading failures of urban rail transit network based on passenger spatiotemporal heterogeneity. Reliab Eng Syst Saf 2024;242:109726. http://dx.doi.org/10.1016/j.ress.2023.109726.

[19] Dui H, Zhang H, Dong X, Zhang S. Cascading failure and resilience optimization of unmanned vehicle distribution networks in IoT. Reliab Eng Syst Saf 2024;246:110071. http://dx.doi.org/10.1016/j.ress.2024.110071.

[20] Wang Y, Zhao O, Zhang L. Multiplex networks in resilience modeling of critical infrastructure systems: A systematic review. Reliab Eng Syst Saf 2024;250:110300. http://dx.doi.org/10.1016/j.ress.2024.110300.

[21] Barabadi A, Ayele Y. Post-disaster infrastructure recovery: Prediction of recovery rate using historical data. Reliab Eng Syst Saf 2018;169:209–23. http://dx.doi.org/10.1016/j.ress.2017.08.018.

[22] Hafeznia H, Stojadinović B. ResQ-IOS: An iterative optimization-based simulation framework for quantifying the resilience of interdependent critical infrastructure systems to natural hazards. Appl Energy 2023;349:121558. http://dx.doi.org/10.1016/j.apenergy.2023.121558.

[23] Wang H, Fang Y-P, Zio E. Resilience-oriented optimal post-disruption reconfiguration for coupled traffic-power systems. Reliab Eng Syst Saf 2022;222:108408. http://dx.doi.org/10.1016/j.ress.2022.108408.

[24] Wang Y, Zhao O, Zhang L. Modeling urban rail transit system resilience under natural disasters: A two-layer network framework based on link flow. Reliab Eng Syst Saf 2024;241:109619. http://dx.doi.org/10.1016/j.ress.2023.109619.

[25] Kim J, ri Yi S, Park J, Kim T. Efficient system reliability-based disaster resilience analysis of structures using importance sampling. J Eng Fluid Mech 2024;150(11):04024081. http://dx.doi.org/10.1061/JENMDT.EMENG-7800, https://ascelibrary.org/doi/abs/10.1061/JENMDT.EMENG-7800.

[26] Lu Q-L, Sun W, Dai J, Schmöcker J-D, Antoniou C. Traffic resilience quantification based on macroscopic fundamental diagrams and analysis using topological attributes. Reliab Eng Syst Saf 2024;247:110095. http://dx.doi.org/10.1016/j.ress.2024.110095, URL https://www.sciencedirect.com/science/article/pii/S0951832024001698.

[27] Dong S, Gao X, Mostafavi A, Gao J, Gangwal U. Characterizing resilience of flood-disrupted dynamic transportation network through the lens of link reliability and stability. Reliab Eng Syst Saf 2023;232:109071. http://dx.doi.org/10.1016/j.ress.2022.109071, URL https://www.sciencedirect.com/science/article/pii/S095183202200686X.

[28] Liu X, Fang Y-P, Zio E. A hierarchical resilience enhancement framework for interdependent critical infrastructures. Reliab Eng Syst Saf 2021;215:107868. http://dx.doi.org/10.1016/j.ress.2021.107868, URL https://www.sciencedirect.com/science/article/pii/S0951832021003872.

[29] Chen H, Zhou R, Chen H, Lau A. Static and dynamic resilience assessment for sustainable urban transportation systems: A case study of Xi 'an, China. J Clean Prod 2022;368:133237. http://dx.doi.org/10.1016/j.jclepro.2022.133237.

[30] Argyroudis SA, Mitoulis SA, Hofer L, Zanini MA, Tubaldi E, Frangopol DM. Resilience assessment framework for critical infrastructure in a multi-hazard environment: Case study on transport assets. Sci Total Environ 2020;714:136854. http://dx.doi.org/10.1016/j.scitotenv.2020.136854.

[31] Aghababaei MTS, Costello SB, Ranjitkar P. Measures to evaluate post-disaster trip resilience on road networks. J Transp Geogr 2021;95:103154. http://dx.doi.org/10.1016/j.jtrangeo.2021.103154.

[32] Hu J, Wen W, Zhai C, Pei S. Surrogate-based decision-making for post-earthquake recovery scheduling and resilience assessment of subway systems considering the effect of infrastructure interdependency. Reliab Eng Syst Saf 2025;256:110781. http://dx.doi.org/10.1016/j.ress.2024.110781, URL https://www.sciencedirect.com/science/article/pii/S0951832024008524.

[33] Arango E, Nogal M, Yang M, Sousa HS, Stewart MG, Matos JC. Dynamic thresholds for the resilience assessment of road traffic networks to wildfires. Reliab Eng Syst Saf 2023;238:109407. http://dx.doi.org/10.1016/j.ress.2023.109407.

[34] Setunge S, Li C, Mcevoy D, Zhang K, Mullett J, Mohseni H, et al. Failure mechanisms of bridge structures under natural hazards. Melbourne, Australia: Bushfire and Natural Hazards CRC; 2018, URL https://shorturl.at/dpuA8.

[35] Andric J, Lu D. Risk assessment of bridges using fuzzy logic controller. In: EURODYN. 2014.

[36] Chan A. Wildfire continues to topple trees onto highway 4 near Port Alberni. 2023, URL https://vancouverisland.ctvnews.ca/wildfire-continues-to-topple-trees-onto-highway-4-near-port-alberni-1.6437721.

[37] McGowan M. Get the trees back': NSW minister wanted 'clearance zone' around highways after bushfires. 2021, URL https://www.theguardian.com/australia-news/2021/feb/25/get-the-trees-back-nsw-minister-wanted-clearance-zone-around-highways-after-bushfires.

[38] FS-USDA. Hazard & danger tree removal. 2023, URL https://www.fs.usda.gov/detail/mthood/fire/?cid=fseprd93747.

[39] Arango E, Nogal M, Sousa HS, Matos JC, Stewart MG. GIS-based methodology for prioritization of preparedness interventions on road transport under wildfire events. Int J Disaster Risk Reduct 2023;99:104126. http://dx.doi.org/10.1016/j.ijdrr.2023.104126.

[40] Rebello K, Jaggi K, Costello S, Blake D, Oo M, Hughes J, et al. Testing a criticality framework for road networks in Auckland, New Zealand. Int J Disaster Resil Built Environ 2020;36, 51. http://dx.doi.org/10.1108/IJDRBE-03-2018-0012.

[41] Carrion C, Levinson D. Value of travel time reliability: A review of current evidence. Transp Res Part A: Policy Pr 2012;46(4):720–41. http://dx.doi.org/10.1016/j.tra.2012.01.003, URL https://www.sciencedirect.com/science/article/pii/S0965856412000043.

[42] San-Miguel-Ayanz J, Boca R, Branco A, de Rigo D. Evaluation of impacts of forest fires in Portugal. Tech. rep. report in support of the european union solidarity fund, JRC Science and Policy Reports; 2018.

[43] DGT. Carta de uso e ocupação do solo para 2018. 2018, URL https://www.dgterritorio.gov.pt/Carta-de-Uso-e-Ocupacao-do-Solo-para-2018.

[44] CTI. análise e apuramento dos factos relativos aos incêndios que ocorreram em pedrógão grande, castanheira de pera, ansião, alvaiázere, figueiró dos vinhos, arganil, góis, penela, pampilhosa da serra, oleiros e sertã, entre 17 e 24 de junho de 2017. Tech. rep., Portugal: Comissao Técnica Independente, Assembleia da República; 2017, URL https://mysl.nl/oYQB.

[45] Duvernay A. Crews clearing holiday fire farm roads: 10,000 trees down, maybe 60,000 to go. 2023, URL https://eu.registerguard.com/story/news/2020/10/04/crews-clear-highway-126-holiday-farm-fire-debris-trees/3589168001/.

[46] Kavanaugh S, Sickinger T. Explosion, sparks from power line preceded Oregon's Holiday Farm fire, area residents say. 2023, URL https://www.oregonlive.com/wildfires/2020/09/explosion-sparks-from-power-line-preceded-oregons-holiday-farm-fire-area-residents-say.html.

[47] Boone R, Hollingsworth H, layer C, Keller CL. In deadly maui fires, many had no warning and no way out. Those who dodged a barricade survived. 2023, URL https://apnews.com/article/hawaii-fires-timeline-maui-lahaina-road-block-c8522222f6de587bd14b2da0020c40e9.

[48] Council of Ministers. 20-30 National plan for integrated rural fire management (EN). Tech. rep. resolution of the council of ministers no. 45-A/2020, Portugal: Presidency of the Council of Ministers; 2020, URL https://dre.pt/dre/en/detail/resolution-of-the-council-of-ministers/45-a-2020-135843143.

[49] Arango E, Nogal M, Jiménez P, Sousa HS, Stewart MG, Matos JC. Policies towards the resilience of road-based transport networks to wildfire events. The Iberian case. Transp Res Procedia 2023;71:61–8. http://dx.doi.org/10.1016/j.trpro.2023.11.058, XV Conference on Transport Engineering, CIT2023.

[50] INE, PORDATA. Número de bombeiros. 2021, URL https://www.pordata.pt/municipios/numero+de+bombeiros-39.

[51] PROCIV. Guia de procedimentos para a constituição e gestão de equipas de intervenção permanente. Tech. rep. 29 cadernos técnicos PROCIV, Portugal: Autoridade nacional de emergência e proteção CIVIL; 2022, URL https://prociv.gov.pt/media/l2kh5bsg/ct_prociv_29-guia-eip_2022.pdf.

[52] Kabai M. Queda de árvore na estrada da praia de faro encerrou trânsito por mais de uma hora. 2022, URL https://www.algarveprimeiro.com/d/queda-de-arvore-na-estrada-da-praia-de-faro-encerrou-transito-por-mais-de-uma-hora/43989-83.

[53] Hawkins S. 2 dead, others hurt after tree falls on California highway during raging storm. 2023, URL https://shorturl.at/anJY5.

[54] Pais. Trânsito esteve três horas cortado na avenida de roma após queda de poste de eletricidade. 2020, URL https://www.dn.pt/pais/transito-cortado-na-avenida-de-roma-em-lisboa-apos-queda-de-poste-de-eletricidade-12912665.html.

[55] OEM. Oregon wildfire response and recovery: What we did in step 2 cleanup. 2023, URL https://wildfire.oregon.gov/Pages/step-2-cleanup.aspx.

[56] Arango E, Nogal M, Yang M, Sousa HS, Stewart MG, et al. Effectiveness assessment of adaptation to build resilient road networks to wildfires. In: ICASP14 proceedings. Dublin, Ireland: ICASP14; 2023, p. 1–8, URL http://hdl.handle.net/2262/103215.